Journal Pre-proof

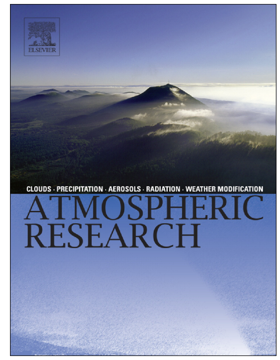

Data assimilation of a dense wind profiler network and its impact on convective forecasting

Cheng Wang, Yaodeng Chen, Min Chen, Jie Shen

PII:	S0169-8095(19)31310-9
DOI:	https://doi.org/10.1016/j.atmosres.2020.104880
Reference:	ATMOS 104880
To appear in:	*Atmospheric Research*
Received date:	21 October 2019
Revised date:	30 January 2020
Accepted date:	31 January 2020

Please cite this article as: C. Wang, Y. Chen, M. Chen, et al., Data assimilation of a dense wind profiler network and its impact on convective forecasting, *Atmospheric Research*(2020), https://doi.org/10.1016/j.atmosres.2020.104880

Data assimilation of a dense wind profiler network and its impact on convective forecasting

Cheng Wang[a], Yaodeng Chen [a,*], Min Chen[b,*], Jie Shen[a]

[a] *Key Laboratory of Meteorological Disaster of Ministry of Education (KLME) / Joint International Research Laboratory of Climate and Environment Change (ILCEC) / Collaborative Innovation Center on Forecast and Evaluation of Meteorological Disasters, Nanjing University of Information Science & Technology, Nanjing 210044, China*

b Institute of Urban Meteorology, CMA, Beijing 100089, China

October 2019

* *Corresponding author:*

Dr. Yaodeng Chen, keyu@nuist.edu.cn

Address: Nanjing University of Information Science & Technology, Nanjing, China, 210044.

Min Chen, mchen@ium.cn

Address: Institute of Urban Meteorology, CMA, Beijing 100089, China

ABSTRACT

Two momentum control variable schemes are typically used in most data assimilation systems: stream function and unbalanced velocity potential (ψ/χ_u $scheme$) and eastward and northward velocity (U/V $scheme$). The wind profiler radar (profiler) plays an important role in the expansion of meteorological observations networks. In this study, the impacts of two momentum control variable schemes on assimilating a dense wind profiler network are discussed based on the single profiler station observation tests and six convective rainfall events cycling experiments.

Single profiler station observation tests indicate that profiler data assimilation is sensitive to control variables. The dynamical increments using U/V $scheme$ contain more elaborate structure, which contributes to valuing the straightforward effects of profiler observations objectively. By contrast, unrealistic increments occur around the observation station in the experiment using ψ/χ_u $scheme$. Six continuous cycling experiments further demonstrate that, for convective rainfall events, experiment using U/V $scheme$ leads to more skillful quantitative precipitation forecasts of convective rainfall. Diagnostic analysis results show that analysis using ψ/χ_u $scheme$ prevents a good fitting to the profiler data, and accurate dynamical analysis containing abundant small-scale disturbances are the main reason for improving precipitation prediction of convective rainfall when U/V $scheme$ is adopted.

Key words: Data assimilation, wind profiler radar observation, momentum control variables, numerical weather prediction.

1 Introduction

As one of modern weather radars, the wind profiler radar (profiler) plays an important role in the development of meteorological observations networks and profiler data can give added details of wind temporally and spatially (St-James and Laroche, 2005). In recent decades, the profiler observation network has been gradually established in many countries, such as the United States, Britain and Germany (Barth et al. 1994; Bouttier, 2001; Benjamin et al. 2004). In China, the profiler radar has been preliminarily developed since the 1980s, mainly concentrated in the Yangtze River Delta, the Pearl River Delta and the Beijing-Tianjin-Hebei District so far. A 225-profiler network has been planned to be established covering the whole country till 2025 (Zhang et al. 2017).

Several evidences suggest that reliable profiler observations can provide reasonable initial fields for numerical weather prediction (NWP). When data from the profiler network was added in data assimilation system, the wind forecasts and overall short-range precipitation predictions were enhanced (Smith and Benjamin. 1993; Benjamin et al. 2004). The assimilation of profiler observations could better analyze the characteristics of the low-level winds in the initial condition, leading to improved precipitation forecasts of both location and intensity (Zhang et al. 2016). Studies also demonstrated the positive effects of assimilating profiler observations on the forecasts of fog (Hu et al. 2017).

In most variational data assimilation systems, the background error covariance is usually processed and simplified by control variable transformations (Barker et al., 2004). Currently, there are mainly two types of momentum control variables used: the stream function and unbalanced velocity potential function (hereafter referred as ψ/χ_u) and eastward and northward velocity (hereafter referred as U/V). Wu and Purser (2002) pointed out that under the geostrophic assumption, the initial condition using ψ/χ_u *scheme* kept an appropriate balance between the wind and mass fields and decreased the spin-up, while more information from observations can be well preserved. However, Xie et al. (2012) revealed that, for a regional analysis, the system of Poisson equations was solved for the conversion from ψ and χ to prognostic variables U and V. As ψ and χ were retrieved from background velocity field with Neumann boundary condition, the inaccurate background could give unreasonable increments and the analysis would be seriously worsened.

Studies (Derber and Bouttier, 1999; Berre, 2000) have shown that the ψ/χ_u *scheme* is more suitable in global and regional data assimilation systems with assimilating large-scale observations. Sun et al. (2016) have added U/V *scheme* in Weather Research and Forecasting Data Assimilation (WRFDA) system, which has been applied in the experiments for seven convective events. The result revealed that, for limited-area and high-resolution radar data assimilation, the U/V *scheme* tended to obtain more appropriate velocity field and improved short-term precipitation prediction. For a squall line case, the evaluation of radial velocity data assimilation using two control variable schemes were carried out, and the ψ/χ_u $scheme$ yielded the analysis with discontinuous winds that degraded precipitation forecasts (Li et al. 2016). Shen et al. (2019) also noted that radial velocity assimilation using the U/V $scheme$ generated more accurate wind analysis and leads to improved track and intensity forecasts for typhoon system compared with the ψ/χ_u $scheme$.

Profiler data is viewed as one of the most crucial observations in the meteorological observation system, because it can well capture the information of wind field with high frequency. The temporal and vertical spatial resolutions of profiler observations reach several minutes and dozens of meters respectively, and thus the measurements are routinely applied in real-time monitoring of wind change with time and height (Lambert et al. 2003; Molod et al. 2015). As wind is main observed and analysis variable, it is especially important to adopt proper momentum control variables so that detailed wind information can be obtained. Previous studies (Sun et al. 2016; Li et al. 2016; Shen et al. 2019) have shown that the assimilation of radar radial velocity is sensitive to control variable scheme, and the U/V $scheme$ can lead to better analysis and precipitation forecast. Both the radial velocity and profiler data can measure dynamical information with high frequency, but the measuring principles and methods of these two kinds of observations are quite different. The sensitivity of momentum control variables may depend on the resolvable scale of the model in a limited area domain. Meanwhile, the effect of assimilating a dense wind profiler network using different control variable scheme need further research. The overarching goal of this article is to investigate the characterization of two momentum control variable schemes and their application to profiler data assimilation and weather prediction.

This article is organized as follows: section 2 introduces the specific schemes of momentum control variables in the assimilation system. The profiler data quality control, the configuration of the overall system and the experiment design used in this study are highlighted in section 3. In section 4, we assimilate observations of single profiler station utilizing two control variable schemes and preliminary assessments of analysis increments are described. In section 5, six convective events are selected for three experiments, and results obtained from sensitivity experiments in terms of qualitative precipitation forecasts are discussed. And detailed analysis and forecast impacts of a serious storm case are presented in section 6. Finally, section 7 provides a summary and draws some conclusions.

2 Schemes of momentum control variables in the assimilation system

The three-dimensional variational (3DVAR) data assimilation is solved by minimizing the following cost function (Lorenc, 1986; Kalnay, 2003):

$$J(\mathbf{x}) = \frac{1}{2}\left[\left(\mathbf{x}-\mathbf{x}^{\mathbf{b}}\right)^{\mathrm{T}}\mathbf{B}^{-1}\left(\mathbf{x}-\mathbf{x}^{\mathbf{b}}\right)+\left(\mathbf{y}_{\mathbf{o}}-\boldsymbol{H}(\mathbf{x})\right)^{\mathrm{T}}\mathbf{R}^{-1}\left(\mathbf{y}_{\mathbf{o}}-\boldsymbol{H}(\mathbf{x})\right)\right], \tag{1}$$

where the $J(\mathbf{x})$, $\mathbf{x}$, $\mathbf{x}^{\mathbf{b}}$, $\mathbf{y}_{\mathbf{o}}$, $\boldsymbol{H}$, $\mathbf{B}$ and $\mathbf{R}$ represent the cost function, the analysis field, the first guess, the observation, the non-linear observation operator, the background error covariance matrix and the observation error covariance matrix, respectively. $\mathbf{B}$ is an extremely huge $10^7 \times 10^7$ matrix, and its inverse $\mathbf{B}^{-1}$ is very difficult to calculate. Hence, the matrix decomposition ($\mathbf{B} = \boldsymbol{U}\boldsymbol{U}^{\mathbf{T}}$) is employed to simplification. $\boldsymbol{U}$ is decomposed background matrix. The transformation of control variable ($\mathbf{x}' = \mathbf{x} - \mathbf{x}^{\mathbf{b}} = \boldsymbol{U}\mathbf{v}$) is commonly applied. Therefore, the formulas (1) is transformed into equation (2):

$$J(\mathbf{v}) = \frac{1}{2}\mathbf{v}^{\mathbf{T}}\mathbf{v} + \frac{1}{2}\left(\mathbf{y}' - \boldsymbol{H}(\boldsymbol{U}\mathbf{v})\right)^{\mathbf{T}} \boldsymbol{R}^{-1}\left(\mathbf{y}' - \boldsymbol{H}(\boldsymbol{U}\mathbf{v})\right), \quad (2)$$

where the vector $\mathbf{v}$ is the control variable, and $\mathbf{y}' = \mathbf{y_o} - \boldsymbol{H}(\mathbf{x}^{\mathbf{b}})$ is the innovation vector. After the transformation, the $\mathbf{B}$ matrix is implicitly given in the control variable operator and does not need to be presented directly.

Nowadays, two momentum control variable schemes are commonly used in the assimilation systems, which are illustrated as follows:

(a) the control variables of the ψ/χ_u *scheme* utilize the stream function (ψ), unbalanced velocity potential (χ_u), unbalanced temperature (T_u), the unbalanced surface pressure (Ps_u) and the pseudo relative humidity (RH_s). The ψ and χ are integral of the dot product of the corresponding wind components (u and v) in model grid space. Note that the control variable transformation between control variable space and model space is decomposed of $u = -\frac{\partial\psi}{\partial y} + \frac{\partial\chi}{\partial x}$ and $v = \frac{\partial\psi}{\partial x} + \frac{\partial\chi}{\partial y}$. The conversion between control variables and model variables may introduce potential negative impacts (Wu et al. 2002; Xie et al. 2012);

(b) the U/V *scheme* uses a set of control variables: the eastward velocity (U), the northward velocity (V), temperature (T), surface pressure (Ps) and pseudo relative humidity (RH_s). These momentum variables are not changed during the conversion from control variable space to the model space (Sun et al. 2016; Li et al. 2016). The direct application of momentum variables (U and V) effectively avoids serious analysis errors by a more straightforward transform compared with the ψ/χ_u $scheme$. The control variables in U/V $scheme$ are regarded of no multivariate correlation, which means these variables can be analyzed independently.

3 Data and experiment design

3.1 The profiler data and quality control

The profiler observations used in this study are hourly averaged horizontal winds, which are obtained from the Meteorological Observation Center (MOC) of China Meteorological Administration (CMA). The profiler station distribution in the inner experimental area is displayed in Figure 1.

The profiler detects horizontal and vertical winds based on the scattering effect of electromagnetic waves by the atmospheric turbulence (Adachi et al. 2005; Haefele and Ruffieux 2015), which is always interfered by factors like the precipitation particles and small-scale air masses in the atmosphere, thus affecting the quality and representativeness of the obtained profiler observations. The NWP model is highly sensitive to erroneous observations and is inclined to converge toward outlier. Hence, the quality control procedure is necessary before profiler data assimilation (Lambert et al. 2003).

Zhang et al. (2017) have developed an effective two-step quality control method composed of blacklisting and outlier elimination. This profiler data quality control procure is employed in this study. The first step of quality control (QC1) applies a blacking list to remove problematic profiler stations with unreliable data. Specifically, the correlation coefficient between the observations and background is compared with a predefined threshold (0.6 without rain and 0.4 with rain). If the station correlation coefficient is smaller than the threshold, all recorded observation from this station will be rejected and the station is removed into the blacklist. The profiler station is reliable when its correlation coefficient value exceeds this fixed threshold, then the second step of the quality control (QC2) can be carried out. QC2 is an outlier rejection method based on the iterated reweight minimum covariance determinant (IRMCD; Cerioli 2010; Zhang et al. 2017), which is applied to evaluate profiler observation points of stations passed QC1. After QC1 and QC2 procedure, the profiler data are assumed to be reliable.

Additionally, if all profiler data with high vertical resolution are assimilated in the model without selection, negative effects will be introduced in analysis due to the significant correlation of the wind fields in the vertical direction, and thus, leading to poor performance of analysis and forecasts. Therefore, the profiler data needs a vertical thinning process before assimilation, then only the wind observations at the model vertical levels are reserved in this article. After the two-step quality control and vertical thinning procedures, the profiler data reserved are considered of high quality and can be applied to data assimilation.

The profiler data at the Beijing station before and after the quality control and the vertical thinning is exhibited in Figure 2, as well as the pilot balloon (PILOT) observations. It is suggested that compared with the PILOT observations, the profiler observations are characterized by the higher vertical resolution, which can provide more detailed diagnostic information of the wind fields. Abnormal winds occur at about 6,500 m and 9,500 m in the initial profiler (WPR-IN) observations, which are effectively eliminated and removed after the profiler quality control (WPR-QC). Meanwhile, the vertical structure of wind fields is remained after the vertical thinning process of the quality-controlled profiler data (WPR-QS), indicating the considerable capability of the vertical thinning in adequately reserves the effective information of the profiler observations and reduces the vertical correlation problems of the data.

3.2 Model settings and experiment design

All experiments performed in this study make use of version 3.9.1 of the Advanced Research Weather Research Forecast Model (WRF- ARW; Skamarock et al. 2008) and its Data Assimilation system (WRFDA; Barker et al. 2004). Two-way and two-domain nest is employed, as is shown in Figure 1. The center of the research area is located at (41.0°N, 122.0°E), and the outer (inner) domain has 301×361 (361×421) grids with 9 km (3 km) horizontal resolution. Each domain is featured with 41 vertical levels, from surface to the 50hPa isobaric top. For the outer domain

(D01), the model physics parameterizations mainly used are as follows: the New-Thompson microphysics parameterization, the Rapid Radiative Transfer Model longwave radiation scheme (RRTM; Mlawer et al. 1997), Dudhia shortwave radiation scheme (Dudhia, 1989), the Monin-Obukhov surface layer scheme, the Noah land surface scheme, the Yonsei University (YSU) PBL parameterization (Hong et al. 2006) and the Kain-Fritsch cumulus parameterization scheme (Kain, 2004). In the inner domain (D02), no cumulus is employed, while other physics schemes are the same as those in the outer domain.

The background error covariance is calculated and estimated based on the National Meteorological Center (NMC) method (Parrish and Derber 1992) and the control variable transformation method (CVT, Derber and Bouttier 1999; Chen et al. 2014). The error statistics are estimated with the differences of 12-h and 24-h forecast valid at the same time during July 1-August 31, 2016. The background error covariance is obtained by the CVT method, using the ψ/χ_u *scheme* and the U/V *scheme* as momentum control variables respectively.

The initial and lateral boundary conditions are interpolated from NCEP Global Forecast System (GFS) analyses and forecasts with horizontal spatial resolution of 0.5 × 0.5 degree. The GTS data are assimilated on the outer domain (D01) while the profiler observations are only considered to be assimilated across the inner domain (D02). Three experiments are designed in Table 1. Large-scale observations are primarily assimilated using ψ/χ_u *scheme* whose benefits have been proven (Derber and Bouttier 1999; Xie et al. 2012), thus the GTS observations are assimilated using ψ/χ_u *scheme* for all experiments on D01 in this study.

The profiler data with high vertical densities using different control variables are assimilated on D02. The control experiment (CTRL) runs without profiler observations assimilated, while the ψ/χ_u *scheme* and the U/V *scheme* are utilized for the profiler data assimilation in the experiments of CV5 and CV7, respectively.

4 Single profiler station observation tests

The single observation test is often applied to illustrate the sensitivity of the control variables scheme. The results of single observation tests (using the ψ/χ_u *scheme* and the U/V *scheme*, respectively) are consistent with the conclusion of previous studies (Xie et al. 2012; Sun et al. 2016). It concluded that the U/V *scheme* decreased the length scale and increased the variance compared with the ψ/χ_u *scheme*. As for the actual assimilation of profiler observations in the study, the entire profile of a single station is used as a record. Single profiler station observation tests are carried out in this section to examine the specific effects of different control variable schemes on analysis.

The background field is derived from the Global Forecast System (GFS) analysis at 1800 UTC 02 August 2017. The single profiler station is located at Panshan (41.27°N, 122.04 °E) in Liaoning Province, the observations information is shown in

Figure 5 (yellow line). With the same background and single-station observations, profiler data assimilation was run using two control variable schemes respectively.

The horizontal wind speed and vector increments (difference between analysis and background) at 500 hPa using the ψ/χ_u *scheme* and the U/V *scheme* are displayed in Figure 3. The positive wind speed increments using the U/V *scheme* have much smaller scale but larger magnitude (Figure 3b) compared to that of using the ψ/χ_u *scheme* (Figure 3a). It could be attributed to the smaller length scale and bigger variance in the U/V *scheme*(Xie et al. 2013). However, the ψ/χ_u *scheme* involves the variable transformation from ψ and χ to U and V, thereby it yields larger length scale and smaller variance during solving the Poisson equations (Xie et al. 2013). Also, the ψ/χ_u *scheme* introduces unrealistic negative increments around positive increment at the observation point. The ψ and χ are obtained from integration of wind components, which retains the features of the wind fields when the system of Poisson equations is solved. More precisely, if the positive (negative) increments appear, unphysical negative (positive) increments will be introduced nearby. This phenomenon has nonphysical meaning and tends to generate analysis errors. Fortunately, it can be avoided in the U/V *scheme* in the actual data assimilation.

Figure 4 shows the cross sections of horizontal wind speed increments through the single profiler station along 122.04 °E, from two control variable schemes. The ψ/χ_u *scheme* (Figure 4a) introduces velocity increments with larger impacted area and smaller magnitude compared to that from the U/V $scheme$. The smoothing effect of the ψ/χ_u $scheme$ is also clearly seen in Figure 4a. A pair of positive increment centers occur around the negative increment center at about the 20-30th levels using the ψ/χ_u $scheme$, because ψ and χ preserve integrals of velocity (U and V). On the contrary, only a stronger negative increment center emerges at the same levels using the U/V $scheme$ in Figure 4b. It is reflected that the U/V $scheme$ can well demonstrate information of the profiler observation itself.

Profiles of the wind speed derived from the observation (OBS), background (FG) and analysis (ANA) by the profiler at Panshan station are compared in Figure 5. The background field has been significantly adjusted and fits observation field well, which reflect the positive effect of assimilating profiler observations. It is found that the U/V $scheme$ can obtain an analysis that fits closer to the profiler observations at most levels than the ψ/χ_u $scheme$.

It can be easily found that velocity increments from different momentum control variable schemes are quite different. The U/V $scheme$ contains smaller-scale feature while the ψ/χ_u $scheme$ may result in analysis errors.

5 Assimilating a dense wind profiler network and precipitation forecasts

This study is tasked with assessing the added value of assimilating profiler observations and the impacts of different momentum control variable schemes on the precipitation forecasts. Six convective rainfall events are selected for data assimilation cycling and forecasting experiments (Table 2). A 6-h spin-up run is conducted using GFS analysis and the output is utilized as the first guess for each experiment. Observations are assimilated with a 3-h interval and then the result is integrated to generate 12-h forecasts at each cycle.

5.1 Cases overview

The synoptic situations are various for selected six cases. The CASE1 is a short-term severe convective system accompanied with thunderstorms and windstorms, and intensive low-level convergence is the direct trigger mechanism of this rainstorm. The CASE2 is a heavy storm rainfall far distant from typhoon, under the combined influence of the weakened typhoon and the western Pacific subtropical high. The squall line happens over North China in the CASE3 and CASE4, with severe convective activities including the short-term heavy rainfall, thunderstorms and local hail storms. The CASE5 is also a local severe convective weather event, along with thunderstorms and heavy winds. Under the combined effects of a high-level trough and a low-level shear line, a convective rainfall event is formed with a large scope of regional precipitation in CASE6. Distributions of the 12-hour accumulated rainfall in the six cases are displayed in Figure 6, obtained from the hourly mixed precipitation analysis of the China Meteorological Administration (CHMPA, Shen et al. 2014).

5.2 Averaged 6-h accumulated precipitation scores

To quantitatively evaluate the contributions on profiler data assimilation and forecasts between different control variable schemes, several categorical and probabilistic verification scores have been used. As this study is focusing on the improvement of a heavy precipitation prediction skill, the verification is performed over the accumulated precipitation area. Based on the hourly rainfall observations of CHMPA, the Threat Score (TS), the Bias Score (BS) and the Fractions Skill Score (FSS) are adopted to verify the short-term quantitative precipitation forecasts for chosen inner domain.

Figure 7 shows the averaged TSs, BSs and the FSSs of the 0-6 h and 6-12 h accumulated precipitation at different forecast leading time in data assimilation cycling experiments for multiple cases aggregated over the 96 forecasts. With respect to the average TSs (Figures 7a-7c), the precipitation forecasts for different thresholds are all enhanced when profiler data is assimilated with both ψ/χ_u $scheme$ and U/V $scheme$. For 3 mm and 45 mm threshold, the differences between CTRL and CV5 (using the ψ/χ_u $scheme$) experiments are slight. Higher values of TSs in CV7 shows more skillful prediction after assimilating profiler observations with the use of the U/V $scheme$.

The Bias Score is greater (less) than 1 when spatial precipitation coverage is overestimated (underestimated). Figure 7d-7f show that the CTRL experiment has a higher bias value than CV5 and CV7 experiments at different leading time for 3 mm, 20 mm and 45 mm thresholds. After profiler data assimilation, over-estimated precipitation is reduced to some extent. Moreover, the BSs reach almost 1.0 for the precipitation threshold of 45 mm over the 6-12 h rainfall forecasts, indicating higher prediction skills.

The FSS is a scoring method recorded by the neighborhood precipitation, influenced by specific neighborhood radius values. The neighborhood radius is 6 km in FSS hereafter. The FSSs show generally similar results (Figure 7g-7i) to the TSs. However, FSSs decrease over the 6-12 h forecast hours at the threshold of 45 mm in the CV5, which are even slightly lower than in the CTRL. Results suggest that effects of profiler data assimilation with the ψ/χ_u $scheme$ can be hardly maintained during later forecast hours, while the U/V $scheme$ shows continuously positive impacts over the entire 12 forecast hours.

In general, it indicates more skillful quantitative precipitation forecasts of cycling profiler data assimilation and forecasts with the U/V $scheme$ than that with the ψ/χ_u $scheme$ at most thresholds over the whole 12 forecast hours.

6 Case study

In this section, the heavy rainfall event of CASE2 on 2-4 August 2017 was selected for further analysis to investigate the detailed impacts of profiler data assimilation using different control variable schemes. It is jointly affected by the low pressure of weakened Typhoon Haitang (No. 1710) and the subtropical high. As a result, the associated precipitation is characterized by a large range of persistent heavy rainfall, which has caught plenty of attention from researchers in recent years. For this case study, the detailed diagnostic analysis was compared and discussed.

6.1 Cost functions and RMSEs

As 3DVAR data assimilation system runs by minimizing the cost function (J), J and its observation term (J_o) was primarily compared in Figure 8. It is worth noting that J_o can reflect the fitting of analysis and observation. As is shown in Figure 8, a better cost function convergence occurred in CV7 experiment using $U/V\ scheme$. Simultaneously, J_o using $U/V\ scheme$ is smaller than that from $\psi/\chi_u\ scheme$, which indicates analysis in CV7 results in a closer fit to observation. Also, it reveals that analysis using $\psi/\chi_u\ scheme$ prevents a good fitting to the profiler data compared with analysis using $U/V\ scheme$.

Meanwhile to gain insight into the fitting of analysis and observation, the average root-mean-square errors (RMSEs) between wind analysis and profiler observations at each profiler station are calculated for U component, V component and wind speed from two experiment at 2100 UTC 02 August 2017 (Figure 9). The CV7 experiment appears to have a smaller RMSEs, which confirms that assimilating a dense profiler network using $U/V\ scheme$ can produce analysis fitting profiler observations well.

6.2 Diagnosis of wind fields

(1) Analysis

The impacts of profiler data assimilation mainly focus on its adjustment to the dynamical field. The analysis increments of the horizontal winds at 850 hPa and 500 hPa after assimilating profiler data using two control variable schemes are presented in Figure 10. The results resemble that of single profiler station tests, producing much smoother increments of velocity in CV5 using the ψ/χ_u $scheme$ (Figures 8a,8c). On the other hand, the CV7 experiment (Figures 10b,10d) using the U/V $scheme$ is featured by adjustments on background with larger magnitudes and smaller horizontal spread, reserving more convective disturbances and maintaining the large-scale balance in the surroundings.

From the cost functions and RMSEs shown by Figure 8 and Figure 9, it is found that the U/V $scheme$ can obtain an analysis that objectively reflects the profiler observation itself than that from the ψ/χ_u $scheme$. As is mentioned previously, the length scale of the U/V $scheme$ is smaller compared to that of the ψ/χ_u $scheme$, which yields much smaller decorrelation distances of the U/V $scheme$. Also, the larger variance of the U/V $scheme$ will preserve more small-scale features and contribute to an analysis fitting closer to the profiler observations, while the ψ/χ_u $scheme$ has a smoother effect and increases the horizontal spread in response to larger length scale and smaller variance. All results demonstrate that the U/V $scheme$ is more appropriate for assimilating a dense wind profiler network in regional convection-permitting data assimilation systems.

(2) Forecast

Figure 11 displays the vertical cross section of 3 h forecast initialized at 2100 UTC 02 August 2017 along 41.6 °N. The assimilation of profiler data (Figure 11b,11c) strengthens the uplift vertical velocity, while there is no distinct ascending motion in CTRL experiment without profiler data assimilation. As is seen in Figure 8, the U/V $scheme$ can obtain an analysis that fits closer to the profiler observations, and the positive impact can be lasted. Assimilation with the U/V $scheme$ is characterized by stronger vertical motion in 3 h forecast than that of using ψ/χ_u $scheme$, which reflects the U/V $scheme$ reserves more small-scale features. It can be concluded that the suitable ascending motion can be provided with the U/V $scheme$ as opposed to that with the ψ/χ_u $scheme$.The stronger vertical velocity will benefit the transport of the mosisture condition in vertical direction.

6.3 Accumulated precipitation

(1) Rainfall distribution

Profiler data assimilation adjusts the dynamical field to improve precipitation predictions from both distribution and intensity. The rainfall observations and the 6 h accumulated precipitation initialized at 2100 UTC 02 August 2017 are presented in Figure 12. Compared to observed heavy rainfall (Figure 10a), the CTRL (Figure 10b) shows a cracked rain band at around 42°N, and heavy rainfall center is located at the southeast of the observed one, with the obviously higher intensity. After assimilating profiler data, the CV5 and CV7 (Figures 12c,12d) both improve the prediction of the rainfall compared with the CTRL. The structure of rainfall belt has been adjusted in the CV5 (Figure 12c) using the ψ/χ_u $scheme$, but the discrete rainfall to the north of 42°N still exits. On the other hand, the CV7 (Figure 12d) using the U/V $scheme$ has complete structure of the rain band at the border between Liaoning and Inner Mongolia, which corresponds well with rainfall observations.

Moreover, there is another rainfall center over the Bohai Sea in CTRL, which is relatively weaker compared with CV5 and CV7. Due to the smoothing effect of the ψ/χ_u $scheme$, the rainfall structure with small thresholds is destroyed. The U/V $scheme$ has more reasonable dynamical analysis and leads to more skillful precipitation prediction. In addition, it should be noted that the heavy rainfall center is enlarged with higher intensity after the profiler data assimilation using both control variable schemes.

(2) Hourly accumulated precipitation scores

Precipitation forecast skills of CTRL, CV5 and CV7 were also evaluated, and the scores of the hourly accumulated precipitation of different thresholds averaged for the inner domain are displayed in Figure 13. The verified scores contain the TSs, the BSs and the FSSs, which are calculated over the 12 h forecast hours during data assimilation cycling with the time interval of 3 hours from 0900 UTC 02 August, 2017 to 0000 UTC 04 August, 2017. The CHMPA was used as observation for verification.

As is shown in Figure 13a-13c, the TSs demonstrate clear improvements of CV5 and CV7 compared with the CTRL throughout the entire forecast period, indicating the positive effects of profiler data assimilation. And the U/V *scheme* leads to greater contribution to precipitation forecasts than the ψ/χ_u *scheme*. Furthermore, the differences of TSs tend to be slight with the increasing forecast hours, which suggests weakening impacts of the initial field on the forecasts. The BSs vary relatively consistent with forecast hours in three experiments. The BSs reveal that profiler data assimilation effectively reduce precipitation forecast deviation with the lowest deviation in the CV7. But for the precipitation of 10 mm, the BSs shows that CTRL and CV7 experiment have better skill compared with CV5 while the there is no significant difference between CTRL and CV7. Besides, the FSSs show consistent results with the TSs. However, the CV5 shows even slightly lower FSS scores than the CTRL over the 9-12 h forecast, while the CV7 indicates continuously higher precipitation skill than the CTRL and CV5.

In brief, the detailed investigation of the selected case reveals that profiler data assimilation modifies the wind fields, provides more realistic dynamical analysis and thereby leads to more skillful precipitation prediction. And the CV7 using the U/V *scheme* further contributes to more accurate wind fields and skillful precipitation than CV5 using the ψ/χ_u *scheme*.

7 Conclusion and discussion

The application of profiler data assimilation is essential as the profiler network provides abundant meteorological data with high vertical resolution. This work aims to evaluate the added value of assimilating a dense wind profiler network with two different momentum control variables (the ψ/χ_u *scheme* and the U/V *scheme*). Thereby single profiler station observation tests and continuous cycling assimilation and forecasting experiments for six rainfall cases were compared and discussed. The main results are concluded as follows.

Single-station observation tests showed that profiler data assimilation was sensitive to control variables. The wind increments using the ψ/χ_u *scheme* had smaller magnitude and larger affected area in terms of horizontal spread. In the experiment using U/V *scheme*, smaller scale dynamical increment was introduced, thereby wind increments valued the straightforward effects of wind observations objectively. On the contrary, when the ψ/χ_u *scheme* was adopted, nonphysical and false increments yielded around the observation station. It is concluded that the U/V *scheme* can decrease potential analysis errors and construct a more elaborate wind field.

Six continuous assimilation and forecasting experiments showed that data assimilation of a dense wind profiler network provided more skillful prediction, the experiment using the U/V *scheme* showed more obvious improvements compared to the experiment using the ψ/χ_u *scheme*. Precipitation skill scores demonstrated that profiler data assimilation using U/V *scheme* significantly contributed to improvement in quantitative precipitation forecasts of convective rainfall. Detailed diagnostic analysis results further revealed that the experiment using U/V *scheme* yielded more accurate dynamical analysis containing abundant realistic small-scale disturbances. Thereby $U/V\ scheme$ showed more skillful precipitation prediction of convective rainfall for both intensity and location especially in short-range (0-6 h) forecasts.

In this study, data assimilation of a dense wind profiler network is distinctly affected by control variables, and the $U/V\ scheme$ is more suitable for high-resolution profiler data assimilation. Over the past years, Doppler radar data has been widely applied to improve the initialization with obvious progress in most operational centers. It remains an issue to combine profiler observations and Doppler radar data effectively, which will be investigated in future works.

Acknowledgements

This work was jointly sponsored by the National Key Research and Development Program of China (2017YFC1502102, 2018YFC1506802) and the National Natural Science Foundation of China (41675102).

Reference

Adachi, A., T. Kobayashi, K.S. Gage, D.A. Carter, L.M. Hartten, W.L. Clark, and M. Fukuda, 2005: Evaluation of Three-Beam and Four-Beam Profiler Wind Measurement Techniques Using a Five-Beam Wind Profiler and Coll ocated Meteorological Tower. J. Atmos. Oceanic Technol., 22, 1167–1180, https://doi.org/10.1175/JTECH1777.1

Barker, D.M., W. Huang, Y. Guo, A.J. Bourgeois, and Q.N. Xiao, 2004: A Three-Dimensional Variational Data Assimilation System for MM5: Implementation and Initial Results. Mon. Wea. Rev., 132, 897–914, https://doi.org/10.1175/1520-0493(2004)132<0897:atvdas>2.0.co;2

Barth, M.F., R.B. Chadwick, and D. W. V. D. Kamp, 1994: Data processing algorithms used by NOAA's wind profiler demonstration network. Annales Geophysicae,12, 518, https://doi.org/10.1007/s00585-994-0518-1

Berre, L., 2000: Estimation of Synoptic and Mesoscale Forecast Error Covariances in a Limited-Area Model. Mon. Wea. Rev., 128, 644–667, https://doi.org/10.1175/1520-0493(2000)128<0644:EOSAMF>2.0.CO;2

Benjamin, S.G., B.E. Schwartz, E.J. Szoke, and S.E. Koch, 2004: The Value of Wind Profiler Data in U.S. Weather Forecasting. Bull. Amer. Meteor. Soc., 85, 1871–1880, https://doi.org/10.1175/BAMS-85-12-1871

Bouttier F, 2001: The use of profiler data at ECMWF. Meteor. Z., 10, 497-510, https://doi.org/10.1127/0941-2948/2001/0010-0497

Cerioli, A., 2010: Multivariate outlier detection with high-breakdown estimators. J. Amer. Stat. Assoc., 105, 147-156, https://doi.org/10.1198/jasa.2009.tm09147

Chen, Y., L. Zeng, X. Huang, H. Wang, Y. Gao and Rizvisrh, 2014: A Study of Latitude-Dependent Background Error Covariance and Its Impacts for Tyhoon Data Assimilation and Forcast. Journal of Tropical Meteorology, 30, 654-662, https://doi.org/10.3969/j.issn.1004-4965.2014.04.006

Chen, Y., X. Chen, L. Zeng, H. Wang and Y. Wang, 2016: Influence of Background Sample Error Simulation on Data Assimilation and Forecast. Plateau Meteorology, 35, 767-776. https://doi.org/10.7522/j.issn.1000-0534.2014.00156

Dudhia, J., 1989: Numerical Study of Convection Observed during the Winter Monsoon Experiment Using a Mesoscale Two-Dimensional Model. J. Atmos. Sci., 46, 3077–3107, https://doi.org/10.1175/1520-0469(1989)046<3077:NSOCOD>2.0.CO;2

Derber, J., and F. Bouttier, 1999: A reformulation of the background error covariance in the ECMWF global data assimilation system. Tellus, 51A, 195-221, https://doi.org/10.3402/tellusa.v51i2.12316

Haefele, A., and D. Ruffieux, 2015: Validation of the 1290 MHz wind profiler at Payerne, Switzerland, using radiosonde GPS wind measurements. Meteorol. Appl., 22, 873-878, https://doi.org/10.1002/met.1507

Hong, S., Y. Noh, and J. Dudhia, 2006: A New Vertical Diffusion Package with an Explicit Treatment of Entrainment Processes. Mon. Wea. Rev., 134, 2318–2341, https://doi.org/10.1175/MWR3199.1

Hu, H., J. Sun, and Q. Zhang, 2017: Assessing the Impact of Surface and Wind Profiler Data on Fog Forecasting Using WRF 3DVAR: An OSSE Study on a Dense Fog Event over North China. Appl. Meteor. Climatol., 56, 1059–1081, https://doi.org/10.1175/JAMC-D-16-0246.1

Lambert, W.C., F.J. Merceret, G.E. Taylor, and J.G. Ward, 2003: Performance of Five 915-MHz Wind Profilers and an Associated Automated Quality Control Algorithm in an Operational Environment. J. Atmos. Oceanic Technol., 20, 1488–1495, https://doi.org/10.1175/1520-0426(2003)020<1488:POFMWP>2.0.CO;2

Lorenc, A. C., 1986. Analysis methods for numerical weather prediction. Q.J.R. Meteorol. Soc. 112, 1177-1194. https://doi.org/10.1002/qj.49711247414

Li, X., M. Zeng, Y. Wang, W. Wang, H. Wu and H. Mei, 2016: Evaluation of two momentum control variable schemes and their impact on the variational assimilation of radarwind data: Case study of a squall line. Adv. Atmos. Sci., 33, 1143-1157, https://doi.org/10.1007/s00376-016-5255-3

Mlawer, E. J., S. J. Taubman, P. D. Brown, M. J. Iacono, and S. A. Clough, 1997: Radiative transfer for inhomogeneous atmosphere: RRTM, a validated correlated-k model for the long wave. J. Geophys. Res., 102, D14. 16663–16682, https://doi.org/10.1029/97JD00237

Molod, A., H. Salmun, and M. Dempsey, 2015: Estimating Planetary Boundary Layer Heights from NOAA Profiler Network Wind Profiler Data. J. Atm os. Oceanic Technol., 32, 1545–1561, https://doi.org/10.1175/JTECH-D-14-00155.1

Kain, J.S., 2004: The Kain–Fritsch Convective Parameterization: An Update. J. Appl. Meteor., 43, 170–181, https://doi.org/10.1175/1520-0450(2004)043<0170:TKCPAU>2.0.CO;2

Kalnay, E., 2002: Atmospheric Modeling, Data Assimilation, and Predictability. Cambridge University Press, 342 pp.

Parrish, D.F. and J.C. Derber, 1992: The National Meteorological Center's Spectral Statistical-Interpolation Analysis System. Mon. Wea. Rev., 120, 1747–1763, https://doi.org/10.1175/1520-0493(1992)120<1747:TNMCSS>2.0.CO;2

Shen, F., D. Xu, J. Min, 2019: Effect of momentum control variables on assimilating radar observations for the analysis and forecast for Typhoon Chanthu (2010). Atmospheric Research. 230, 104622, https://doi.org/10.1016/j.atmosres.2019.104622

Shen, Y., P. Zhao, Y. Pan, J. Yu, 2014: A high spatiotemporal gauge-satellite merged precipitation analysis over China. J. Geophys. Res.: Atmos. 119, 3063–3075. https://doi.org/10.1002/2013JD020686

Smith, T.L., and S.G. Benjamin, 1993: Impact of Network Wind Profiler Data on a 3-h Data Assimilation System. Bull. Amer. Meteor. Soc., 74, 801–808, https://doi.org/10.1175/1520-0477(1993)074<0801:IONWPD>2.0.CO;2

Skamarock, W.C., and Coauthors, 2008: A description of the Advanced Research WRF version 3. NCAR Technical note-475+ STR[J]. https://dx.doi.org/10.5065/D68S4MVH

St-James, J.S. and S. Laroche, 2005: Assimilation of Wind Profiler Data in the Canadian Meteorological Centre's Analysis Systems. J. Atmos. Oceanic Technol., 22, 1181–1194, https://doi.org/10.1175/JTECH1765.1

Sun, J., H. Wang, W. Tong, Y. Zhang, C. Lin, and D. Xu, 2016: Comparison of the Impacts of Momentum Control Variables on High-Resolution Variational Data Assimilation and Precipitation Forecasting. Mon. Wea. Rev., 144, 149–169, https://doi.org/10.1175/MWR-D-14-00205.1

Wu, W., R.J. Purser, and D.F. Parrish, 2002: Three-Dimensional Variational Analysis with Spatially Inhomogeneous Covariances. Mon. Wea. Rev., 130, 2905–2916, https://doi.org/10.1175/1520-0493(2002)130<2905:TDVAWS>2.0.CO;2

Xie, Y., and A. E. MacDonald, 2012: Selection of momentum variables for a three-dimensional variational analysis. Pure Appl. Geophys. 169, 335–351. https://doi.org/10.1007/s00024-011-0374-3

Zhang, X., Y. Luo, Q. Wan, W. Ding, and J. Sun, 2016: Impact of Assimilating Wind Profiling Radar Observations on Convection-Permitting Quantitative Precipitation Forecasts during SCMREX. Wea. Forecasting, 31, 1271–1292, https://doi.org/10.1175/WAF-D-15-0156.1

Zhang, Y., M. Chen, and J. Zhong, 2017: A Quality Control Method for Wind Profiler Observations toward Assimilation Applications. J. Atmos. Oceanic Technol., 34, 1591–1606, https://doi.org/10.1175/JTECH-D-16-0161.1

Figure captions

Table 1. The set-up of data assimilation experiments.

Table 2. Six rainfall cases for data assimilation cycling experiments

Figure 1. The study area and the profiler distribution inside.

Figure 2. Comparisons between the profiler data and the PILOT horizontal winds (half barb =2 m/s; barb =4 m/s; flag =20 m/s) at the Beijing station (0000 UTC 18 July 2018). WPR-IN, WPR-QC and WPR-QS refer to the initial profiler observations, the quality-controlled profiler observations and the quality-controlled with vertical thinning profiler observations, respectively. PILOT represents the pilot balloon observations.

Figure 3. Wind analysis increments at level 25 from a single profiler station assimilation; (a) CV5 using the ψ/χ_u scheme, (b) CV7 using the U/V scheme (unit: m/s).

Figure 4. The cross sections of horizontal wind speed analysis increments from a single profiler station assimilation along 122.04 °E; (a) CV5 using the ψ/χ_u scheme, (b) CV7 using the U/V scheme (unit: m/s).

Figure 5. Comparison of the wind speed profiles derived from the observation (OBS), background (FG) and analysis (ANA) at the profiler at Panshan station (41.27°N, 122.04 °E); with (a) CV5 using the ψ/χ_u scheme and (b) CV7 using the U/V scheme (unit: m/s).

Figure 6. The 12-hour accumulated observed precipitation (unit: mm) for the six convective rainfall cases.

Figure 7. The averaged TSs (a-c), BSs (d-f) and FSSs (g-i) for the 0-6 h and 6-12 h accumulated precipitation thresholds of 3mm, 20mm and 45 mm aggregated over 96 forecasts for the 6 rainfall cases, from the CTRL (gray), CV5 (blue) and CV7 (red) experiments (unit: m/s).

Figure 8. The cost function (J) and the observation term (J_o) for CV5 using ψ/χ_u *scheme* (blue lines) and CV7 using U/V *scheme* (red lines) at 2100 UTC 02 August 2017.

Figure 9. The Root-mean-square error of analysis against profiler observations for CV5 using ψ/χ_u *scheme* (blue lines) and CV7 using U/V *scheme* (red lines) at 2100 UTC 02 August 2017. (a) U component, (b) V component, (c) Wind speed; (unit: m/s).

Figure 10. Horizontal analysis increments of the horizontal wind speed fields at (a, b) 850 hPa and (c, d) 500 hPa on the profiler data assimilation with (a, c) CV5 using the ψ/χ_u scheme and (b, d) CV7 using the U/V scheme at 2100 UTC 02 August 2017. The shaded and the vector arrow length both refer to the magnitude of wind increments (unit: m/s).

Figure 11. Vertical Cross sections along 41.6 °N of 3 h forecast initialized at 2100 UTC 02 August 2017; 2D wind vectors (vectors; units: m/s) and vertical velocity

(shaded: 10-1 m/s): (a) CTRL, (b) CV5 using the ψ/χ_u scheme, (c) CV7 using the U/V scheme.

Figure 12. The observed rainfall and forecasts of 6-h accumulated precipitation (unit: mm) from 2100 UTC 02 August 02 to 0300 UTC 03 August,2017 for different experiments. (a) OBS, (b) CTRL, (c) CV5 and (d) CV7.

Figure 13. Verification scores for the hourly accumulated precipitation forecasts averaged over all forecast hours with precipitation thresholds of 2mm, 5mm and 10 mm from the CTRL (black), CV5 (blue) and CV7 (red) experiments. (a-c) TSs, (d- f) BSs and (g-i) FSSs.

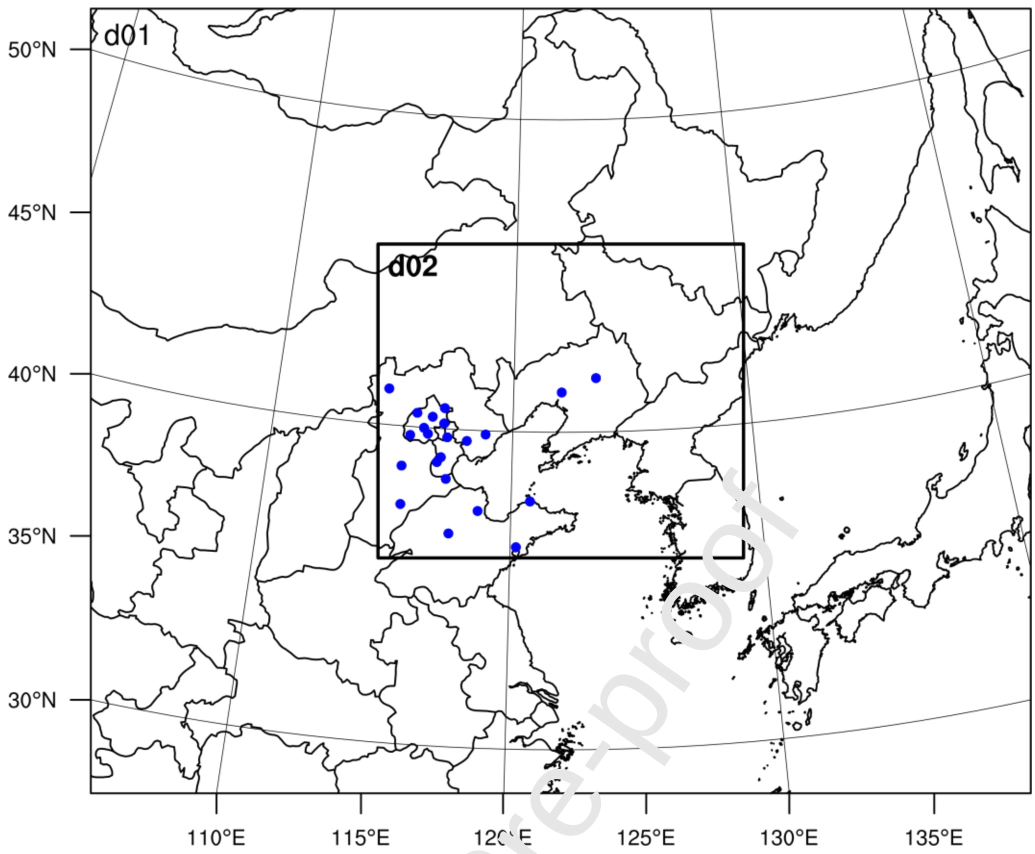

Figure 1. The study area and the profiler distribution inside.

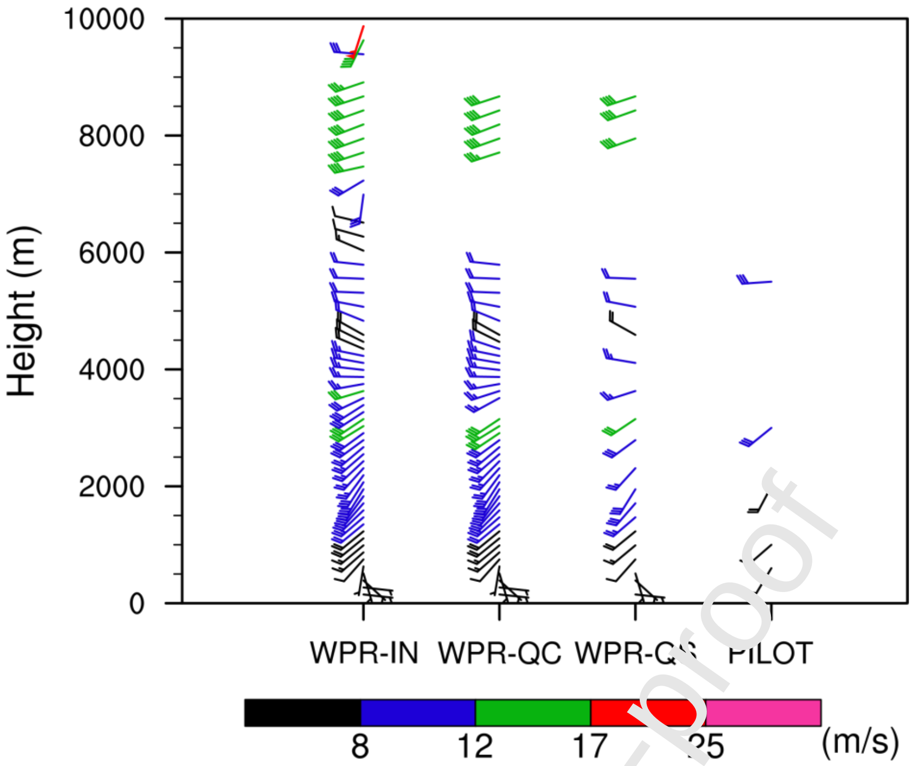

Figure 2. Comparisons between the profiler data and the PILOT horizontal winds (half barb =2 m/s; barb =4 m/s; flag =20 m/s) at the Beijing station (0000 UTC 18 July 2018). WPR-IN, WPR-QC and WPR-QS refer to the initial profiler observations, the quality-controlled profiler observations and the quality-controlled with vertical thinning profiler observations, respectively. PILOT represents the pilot balloon observations.

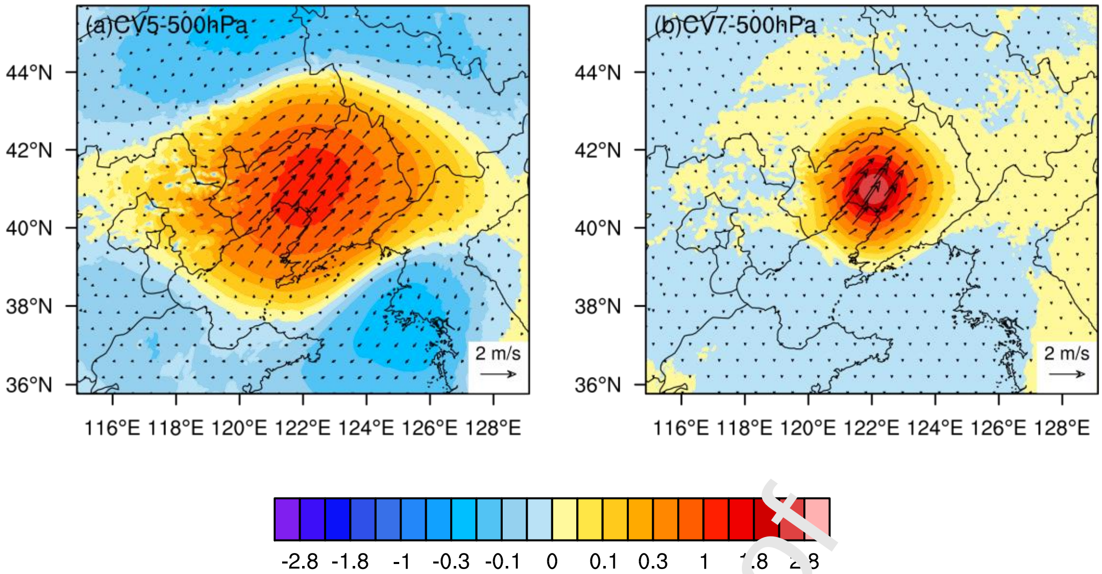

Figure 3. Wind analysis increments at 500 hPa from a single profiler station assimilation; (a) CV5 using the ψ/χ_u scheme, (b) CV7 using the U/V scheme (unit: m/s).

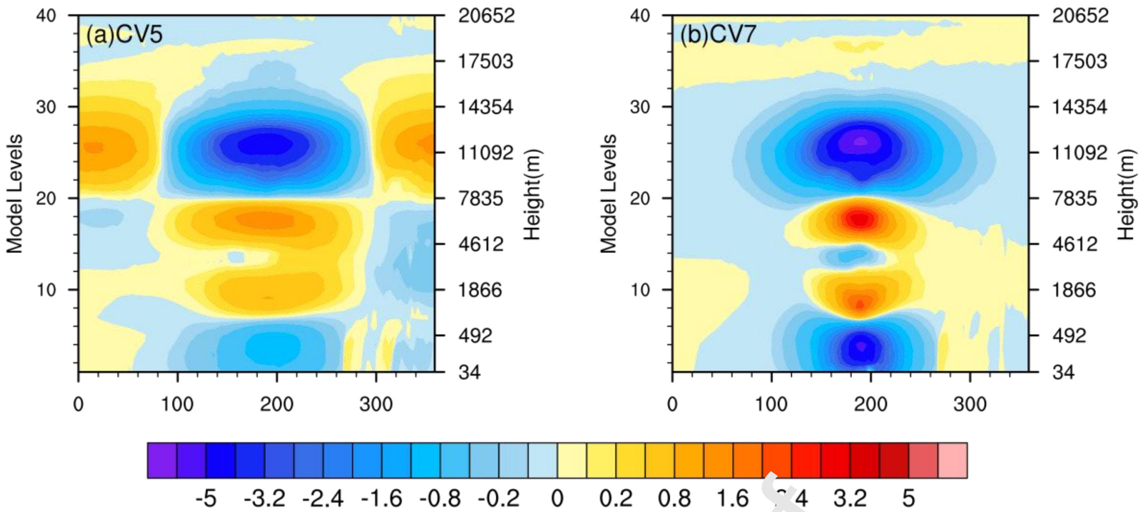

Figure 4. The cross sections of horizontal wind speed analysis increments from a single profiler station assimilation along 122.04 °E; (a) CV5 using the ψ/χ_u scheme, (b) CV7 using the U/V scheme (unit: m/s).

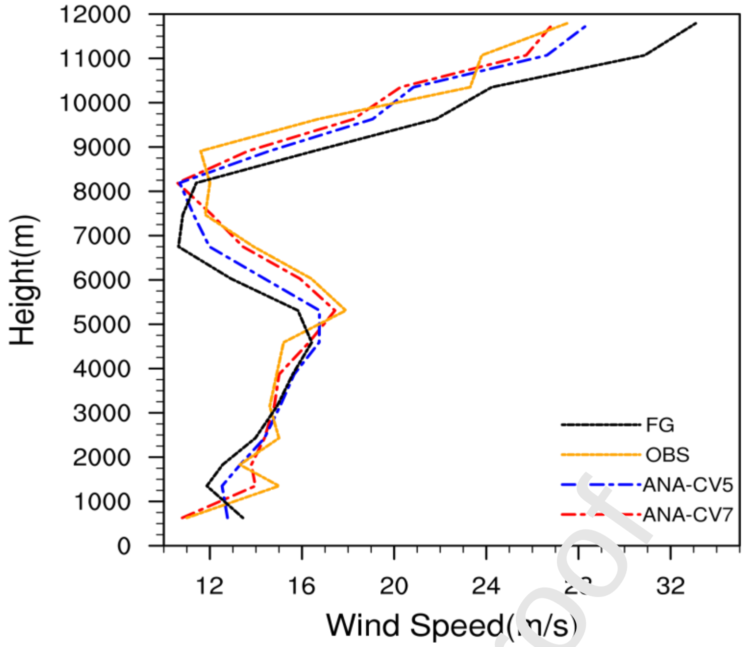

Figure 5. Comparison of the wind speed profiles derived from the observation (OBS), background (FG) and analysis (ANA) at the profiler at Panshan station (41.27°N, 122.04 °E) ; with (a) CV5 using the ψ/χ_u scheme and (b) CV7 using the U/V scheme (unit: m/s).

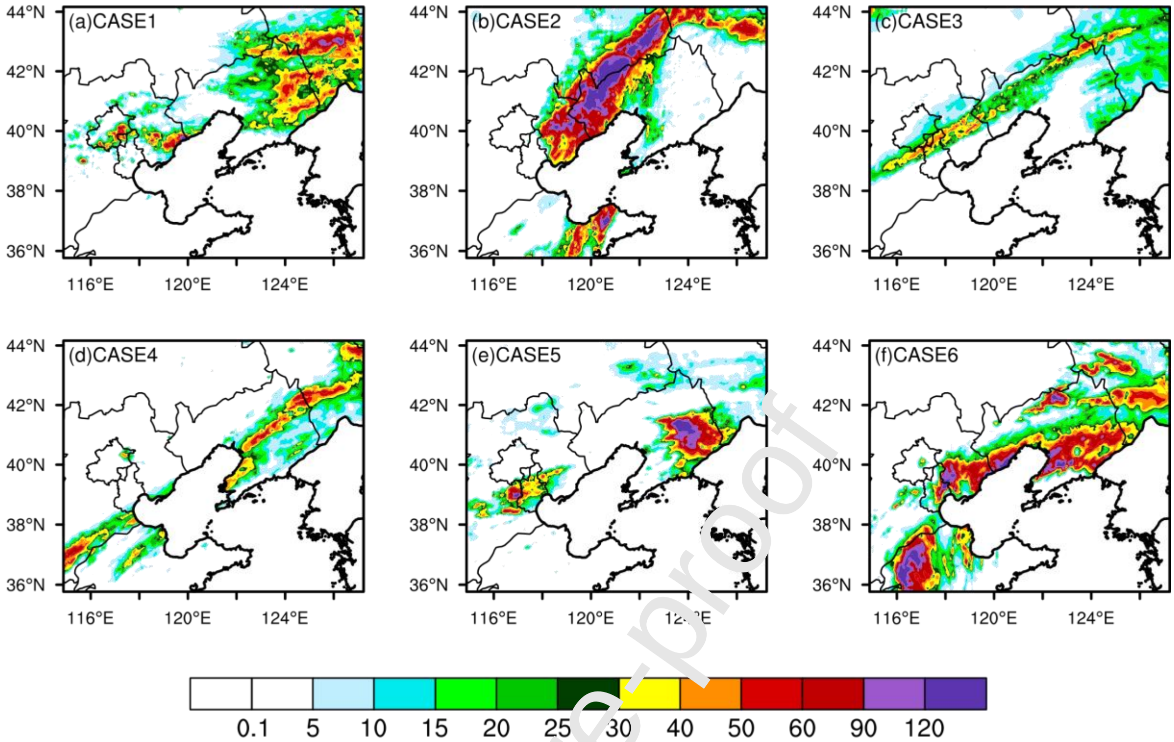

Figure 6. The 12-hour accumulated observed precipitation (unit: mm) for the six convective rainfall cases.

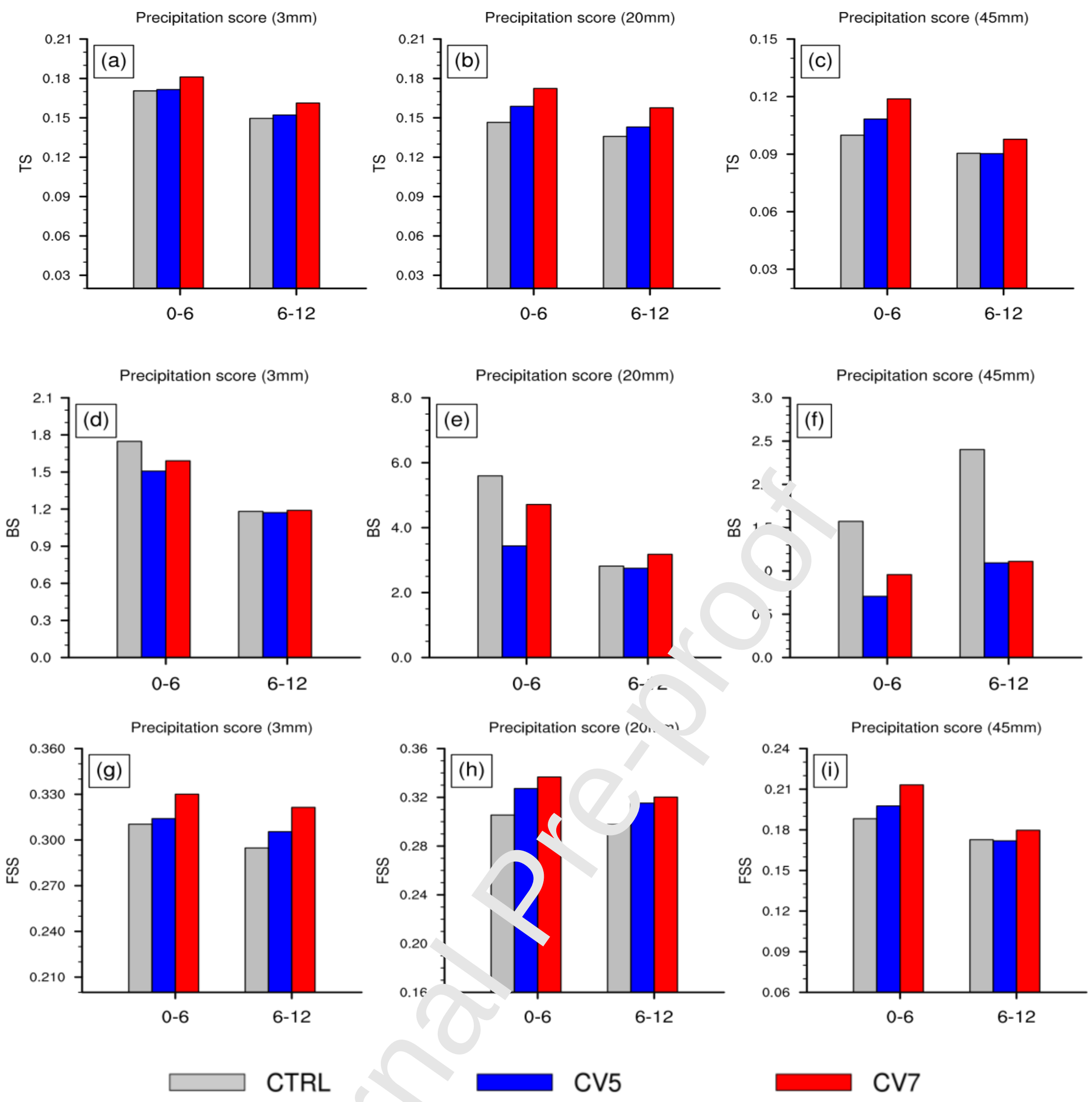

Figure 7. The averaged TSs (a-c), BSs (d-f) and FSSs (g-i) for the 0-6 h and 6-12 h accumulated precipitation thresholds of 3mm, 20mm and 45 mm aggregated over 96 forecasts for the 4 rainfall cases, from the CTRL (gray), CV5 (blue) and CV7 (red) experiments (unit: m/s).

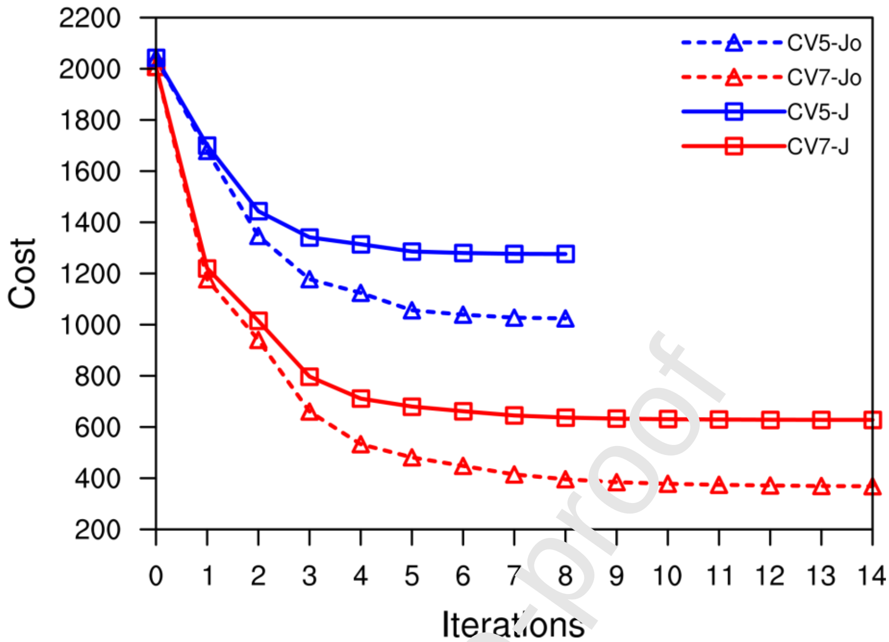

Figure 8. The cost function (J) and the observation term (J_o) for CV5 using ψ/χ_u *scheme* (blue lines) and CV7 using U/V *scheme* (red lines) at 2100 UTC 02 August 2017.

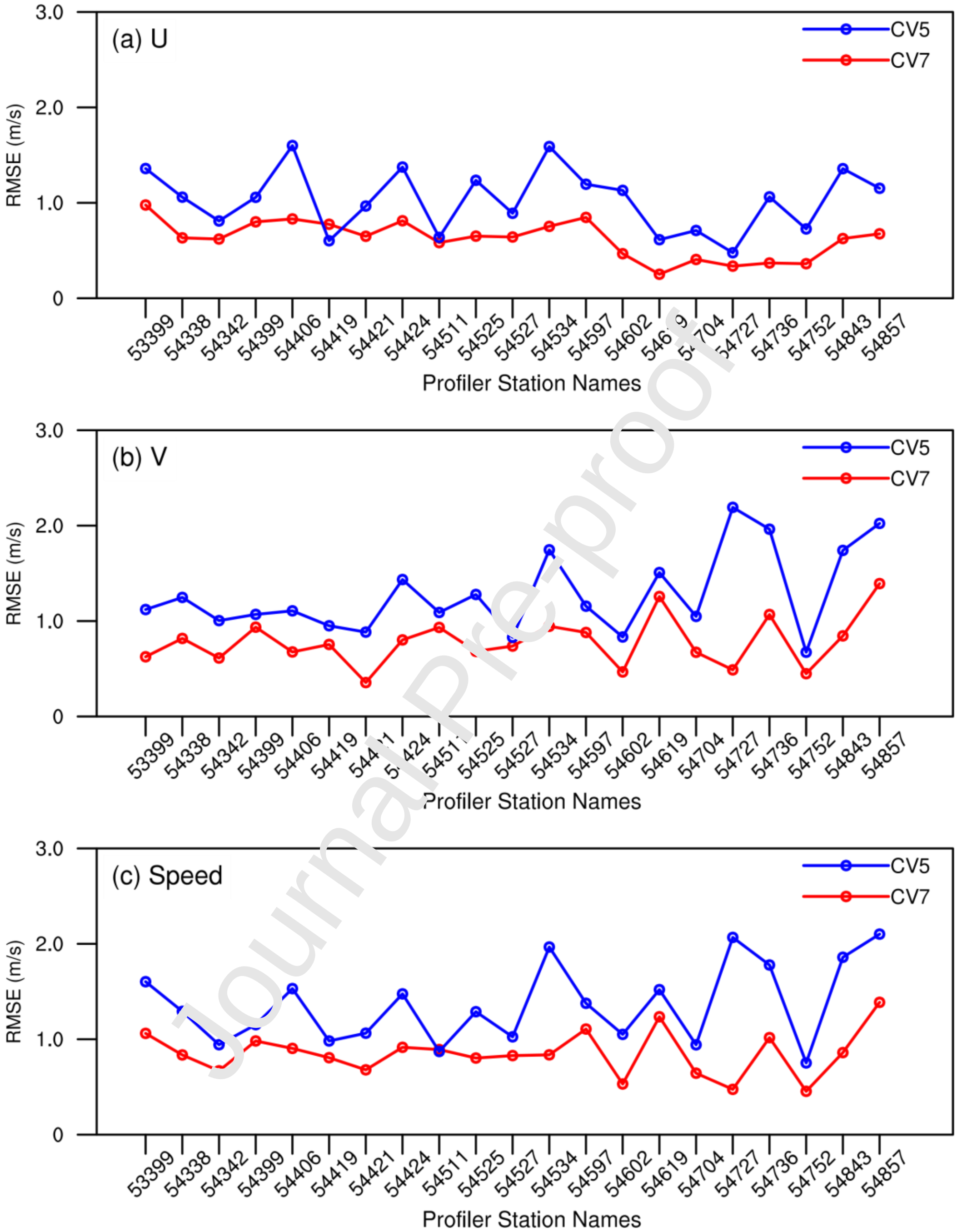

Figure 9. The Root-mean-square error of analysis against profiler observations for CV5 using ψ/χ_u *scheme* (blue lines) and CV7 using U/V *scheme* (red lines) at 2100 UTC 02 August 2017. (a) U component, (b)V component, (c) Wind speed; (unit: m/s).

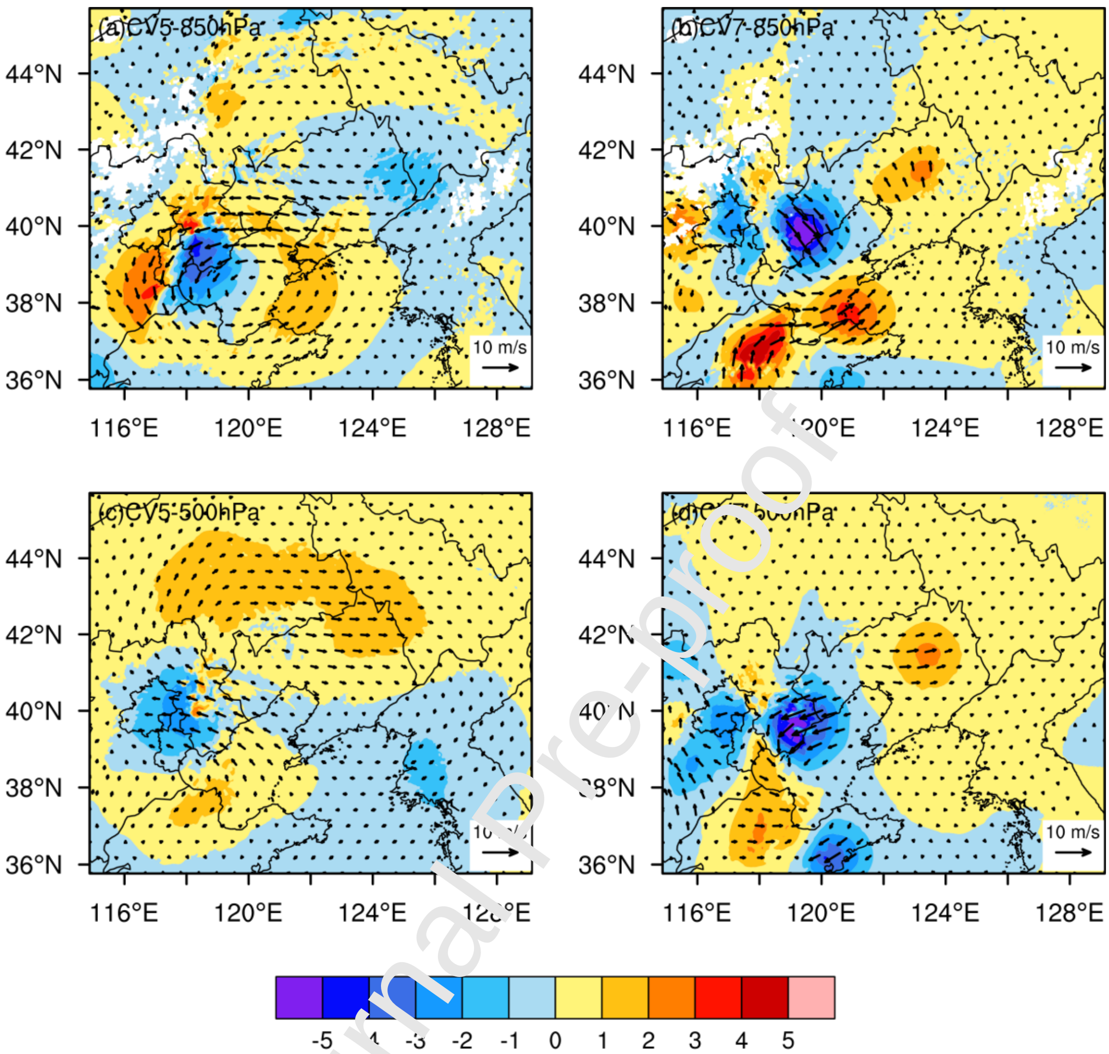

Figure 10. Horizontal analysis increments of the horizontal wind speed fields at (a, b) 850 hPa and (c, d) 500 hPa on the profiler data assimilation with (a, c) CV5 using the ψ/χ_u scheme and (b, d) CV7 using the U/V scheme at 2100 UTC 02 August 2017. The shaded and the vector arrow length both refer to the magnitude of wind increments (unit: m/s).

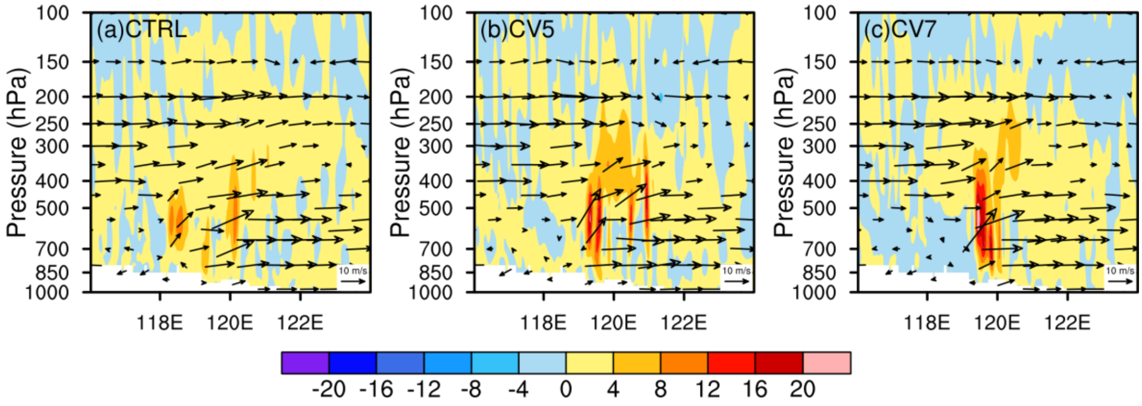

Figure 11. Vertical Cross sections along 41.6 °N of 3 h forecast initialized at 2100 UTC 02 August 2017; 2D wind vectors (vectors; units: m/s) and vertical velocity (shaded: 10-1 m/s): (a) CTRL, (b) CV5 using the ψ/χ_u scheme, (c) CV7 using the U/V scheme.

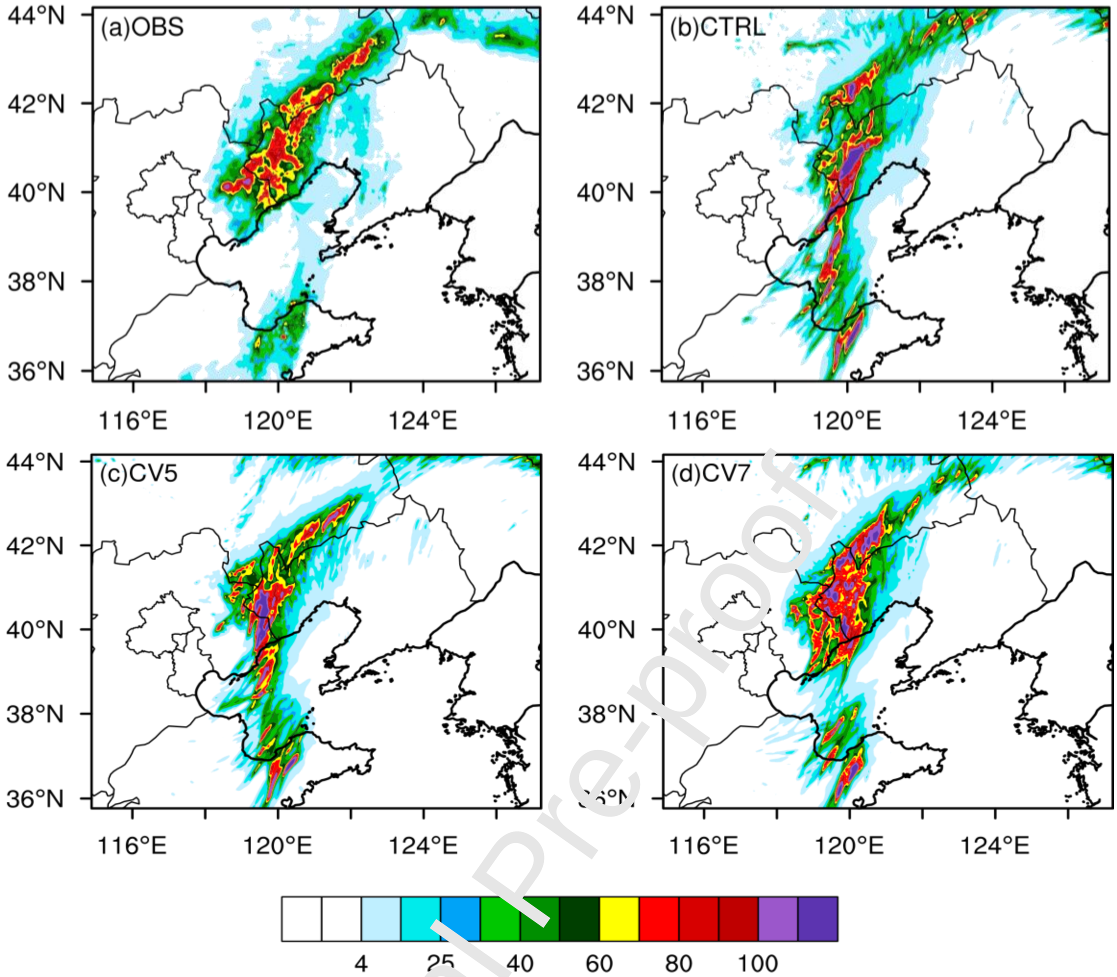

Figure 12. The observed rainfall and forecasts of 6-h accumulated precipitation (unit: mm) from 2100 UTC 02 August 02 to 0300 UTC 03 August,2017 for different experiments. (a) OBS, (b) CTRL, (c) CV5 and (d) CV7.

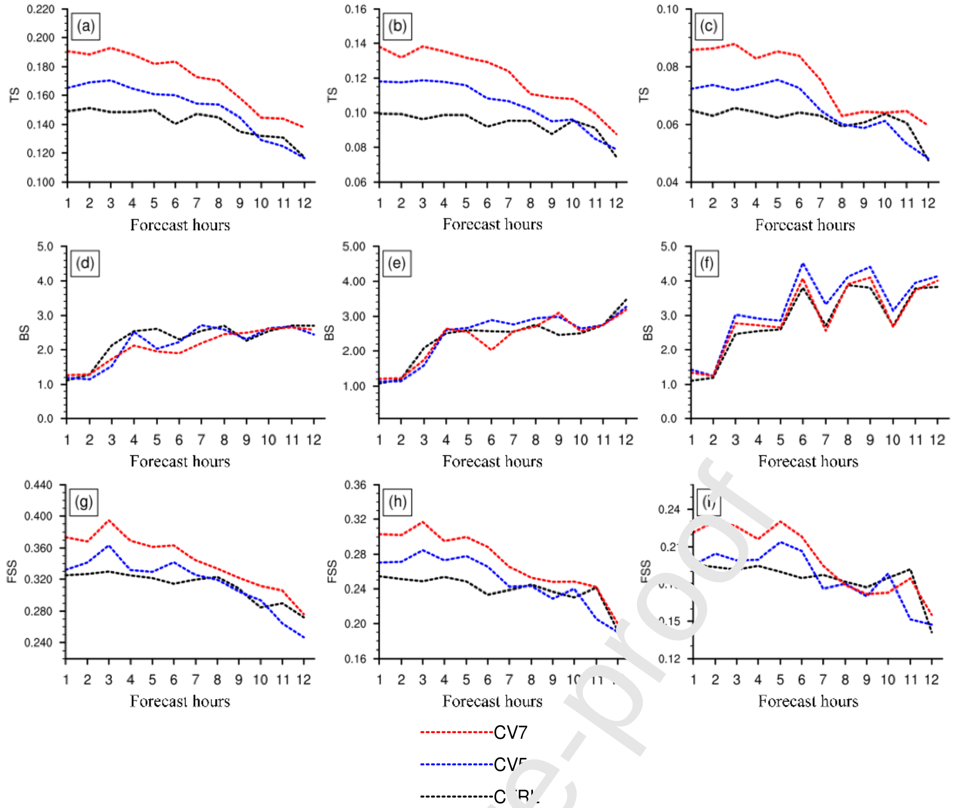

Figure 13. Verification scores for the hourly accumulated precipitation forecasts averaged over all forecast hours with precipitation thresholds of 2mm, 5mm and 10 mm from the CTRL (black), CV5 (blue) and CV7 (red) experiments. (a-c) TSs, (d-f) BSs and (g-i) FSSs.

Table 1. The set-up of data assimilation experiments

Experiment	D01 Domain	D02 Domain
CTRL	GTS observations using ψ/χ_u scheme,	No profiler data assimilation.
CV5	GTS observations using ψ/χ_u scheme,	Profiler observations using ψ/χ_u scheme.
CV7	GTS observations using ψ/χ_u scheme,	Profiler observations using U/V scheme.

Table 2. Six rainfall cases for data assimilation cycling experiments

Case	Date
CASE1	Start: 0600 UTC 18 July, 2017 End: 0000 UTC 20 July, 2017
CASE2	Start: 0600 UTC 2 August, 2017 End: 0000 UTC 4 August, 2017
CASE3	Start: 0600 UTC 10 July, 2018 End: 0000 UTC 12July, 2018
CASE4	Start: 0600 UTC 13 July, 2018 End: 0000 UTC 15 July, 2018
CASE5	Start: 1200 UTC 4 August, 2018 End: 1200 UTC 7 August, 2018
CASE6	Start: 0600 UTC 13 August, 2018 End: 0600 UTC 15 August, 2018

Author Statement

Cheng Wang: Conceptualization, Methodology, Formal analysis, Writing-Original draft, Visualization, Validation

Yaodeng Chen: Conceptualization, Methodology, Funding acquisition, Resources, Supervision, Writing-review & editing, Validation

Min Chen: Methodology, Data curation, Supervision, Validation

Jie Shen: Visualization, Writing-review & editing, Validation

Declaration of interests

☒ The authors declare that they have no known competing financial interests or personal relationships that could have appeared to influence the work reported in this paper.

☐ The authors declare the following financial interests/personal relationships which may be considered as potential competing interests:

Highlights

(1) Single-station observation tests indicate that profiler data assimilation is sensitive to control variables. The analysis of tests using $U/V\ scheme$ contains more elaborate structure which reflects the characteristics of high-resolution profiler observation.

(2) Six convective rainfall events cycling experiments show that the $U/V\ scheme$ can obtain more accurate wind analysis from profiler and leads to more skillful precipitation prediction.

(3) Diagnostic analysis results show that accurate dynamical analysis containing abundant small-scale disturbances are the main reason for improving precipitation prediction of convective rainfall when $U/V\ scheme$ is adopted.